Computation of Causal Characteristic Impedances

Dylan F. Williams, *Senior Member, IEEE,* and Ronald C. Wittmann, *Senior Member, IEEE*
National Institute of Standards and Technology, 325 Broadway, Boulder, CO 80303
Ph: [+1] (303)497-3138 Fax: [+1] (303)497-3122 E-mail: dylan@boulder.nist.gov

***Abstract*- We develop a numerical method of determining the magnitude of characteristic impedance required by causal power-normalized circuit theories from its phase using a Hilbert-transform relationship. We also estimate the uncertainty in the method.**

INTRODUCTION

We develop a numerical algorithm for computing the magnitude of the characteristic impedance $Z_0(\omega)$ required in the causal power-normalized waveguide circuit theory of [1] from its phase. We determined the phase of Z_0 from an integral of the Poynting vector over the cross section of the guides, as required by the power normalization of [1], using the full-wave method of [2]. We assess the error of the algorithm, which uses a Hilbert-transform relationship to determine the magnitude of Z_0 from its phase.

The causal waveguide circuit theory of [1] marries the power normalization of [3] and [4] with additional constraints that enforce simultaneity of the theory's voltages and currents and the actual fields in the circuit. These additional constraints not only guarantee that the network parameters of passive devices in this theory are causal, but they determine the characteristic impedance $Z_0(\omega)$ of a single-mode waveguide within a positive frequency-independent multiplier. References [5] and [6] examine some of the implications of [1], determining the characteristic impedance required by that theory in a lossless coaxial waveguide, a lossless rectangular waveguide, an infinitely wide metal-insulator-semiconductor transmission line, and microstrip lines on silicon substrates.

In this paper we discuss the numerical method used in [5] and [6] to determine the characteristic impedance required by the causal power-normalized circuit theory of [1], and estimate the uncertainty in $|Z_0|$ caused by errors in its phase. We test the estimates with a Monte-Carlo experiment.

CAUSAL CHARACTERISTIC IMPEDANCE

The complex power p_+ carried by the forward mode is given by an integral of the Poynting vector over the cross section of the guide:

$$p_+(\omega,z) \equiv \int \boldsymbol{E}_t(\omega,\boldsymbol{r},z)\times\boldsymbol{H}_t^*(\omega,\boldsymbol{r},z)\cdot\hat{\boldsymbol{z}}\,\mathrm{d}\boldsymbol{r}, \qquad \textbf{(1)}$$

where ω is the angular frequency, z is the longitudinal coordinate, $\hat{\boldsymbol{z}}$ is the unit vector in the direction of propagation, $\boldsymbol{r} = (x,y)$ is the transverse position vector, and $\boldsymbol{E}_t$ and $\boldsymbol{H}_t$ are the transverse electric and magnetic fields. The power normalization of the circuit theories of [3] and [4] require that the phase angle of Z_0 be set equal to the phase of p_+, which from **(1)** is independent of z and is a fixed property of the guide: that is, they require $\arg(Z_0(\omega)) = \arg(p_+(\omega)) \equiv \arg(p_+(\omega,0)) = \arg(p_+(\omega,z))$. This condition on the phase of Z_0 is a direct consequence of the power-normalization of the circuit theories, and is required to ensure that the time-averaged power in the guide is equal to the product of the voltage and the conjugate of the current [3].

The causal circuit theory of [1] imposes the same power normalization, so $\arg(Z_0) = \arg(p_+)$. In addition,

that theory requires that Z_0 be minimum phase. That is, [1] requires

$$\mathcal{H}\left(\ln|Z_0(\omega)|\right) = \arg[p_+(\omega)], \qquad \textbf{(2)}$$

where $\mathcal{H}$ is the Hilbert transform. This condition ensures that voltage (or current) excitations in the guide do not give rise to a current (or voltage) response before the excitation begins.

Once $\arg(p_0)$ is determined by the power condition **(1)**, the space of solutions for $|Z_0|$ is defined by

$$|Z_0(\omega)| = \lambda e^{-\mathcal{H}(\arg[p_+(\omega)])}, \qquad \textbf{(3)}$$

where λ is a real positive frequency-independent constant that determines the overall impedance normalization [1]. Eqn. **(3)** results from two facts: the Hilbert transform has a null space consisting of the constant functions, and $\mathcal{H}[\mathcal{H}[f(\omega)]] = -f(\omega) + c$, where c is a real frequency-independent constant.

NUMERICAL CALCULATION OF $|Z_0|$

To determine $|Z_0|$, we use the full-wave method of [2] to calculate $\arg(p_+)$ and a discrete Hilbert transform to calculate $|Z_0|$ from **(3)**. For many quasi-TEM guides incorporating lossless dielectrics, Z_0 approaches $\sqrt{R/j\omega C}$ at low frequencies, and $\arg(p_+)$ approaches $\pm\pi/4$ as ω approaches 0. If this is the case, we choose the parameter a so that the function

$$\frac{\pm\pi/4}{1 + a|\omega|/8} \qquad (\omega \gtrless 0) \qquad \textbf{(4)}$$

is nearly equal to $\pi/4$ at the low frequencies and is small at the high frequencies we are interested in. Then we add **(4)** to $\arg(p_+)$, eliminating the discontinuity at ω=0, perform the discrete Hilbert transform in **(3)**, and subtract the function

$$\frac{1}{2\left[1 - (a\omega/8)^2\right]} \ln\left|\frac{a\omega}{8}\right|, \qquad \textbf{(5)}$$

which, with the aid of [7], can be shown to be the Hilbert transform of **(4)**.

Because the calculations of $\arg(p_+)$ are time consuming, we determine $\arg(p_+)$ at only a limited number of frequency points. However, the numerical algorithm requires that the input data be uniformly spaced in frequency, so we add data points with $\arg(p_+)$ and its derivative equal to 0 at ω=0 and $\omega=\omega_1$ to the set of $\arg(p_+)$, where ω_1 is much larger than the largest frequency at which we calculated $\arg(p_+)$, and use a cubic spline to interpolate $\arg(p_+)$ over the entire frequency range.

HIGH-FREQUENCY ERRORS

During the interpolation procedure, we assumed that $\arg(p_+)$ approached 0 smoothly outside of the region in which we performed full-wave calculations, while $\arg(p_+)$ may in fact display a complicated behavior at high frequencies. In addition, the periodic extension implicit in the discrete Hilbert transform may introduce additional high-frequency error in $\arg(p_+)$. Because the Hilbert transform is not a local transform, errors in $\arg(p_+)$ at these high frequencies will create errors in the calculated magnitude of Z_0 at lower frequencies.

Appendix 4 of [1] develops a bound for the error in $|Z_0|$ at a given frequency ω when the $\arg(p_+)$ is known exactly up to some greater frequency ω_0, but is unknown above ω_0. The result is

$$\frac{\omega_0^2 - \omega^2}{\omega_0^2} \le \left|\frac{Z_0'(\omega)}{Z_0(\omega)}\right| \le \frac{\omega_0^2}{\omega_0^2 - \omega^2}, \qquad \textbf{(6)}$$

where Z_0 is the actual characteristic impedance and Z_0' is the value of characteristic impedance we determine from incorrect assumptions about the high-frequency behavior of $\arg(p_+)$ above ω_0.

Figure 1 illustrates the algorithm applied to the 5-µm wide microstrip lines on a 1 µm thick oxide layer supported by a 100 Ω·cm silicon substrate described in [6]. In this case we chose λ so as to match $|Z_0'|$ and the

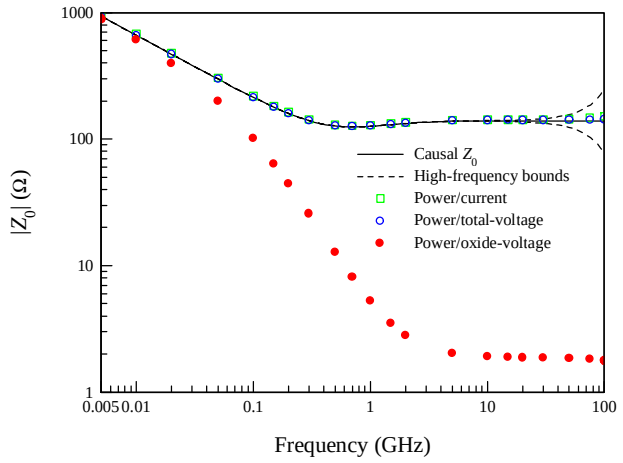

Fig. 1. The magnitude of Z_0 determined with different definitions for the 5-μm wide microstrip lines on a 100 Ω-cm silicon substrate described in [6]. The bounds were determined from **(6)** with ω_0 = 150 GHz.

magnitude of the power/total-voltage characteristic impedance at 0.005 GHz, the lowest frequency at which we performed full-wave calculations. The figure compares the causal result calculated with the algorithm described in this work (solid line) to the conventional power/total-voltage (circles) and power/center-conductor-current definitions (squares) discussed in [6], and shows that the agreement with these conventional definitions is good.

Fig. 1 also shows the characteristic impedance calculated from the power/oxide-voltage definition discussed in [6] in solid circles. Here the voltage path used to define Z_0 extended from the bottom of the microstrip signal conductor through the oxide to the surface of the silicon substrate. We argued in [6] that the discrepancies between this definition and the causal calculation are large enough to conclude that the power/oxide-voltage definition cannot be causal.

Fig. 1 shows in dashed lines the error bounds from **(6)** calculated with ω_0 = 150 GHz. These bounds limit the maximum error we could have made in our calculation of the causal Z_0 caused by unexpected behavior in arg(p_+) above 150 GHz. The bounds indicate that the differences between the causal and power/oxide-voltage definitions cannot be attributed to unexpected high-frequency behavior of arg(p_+), confirming the conclusion of [6]: the power/oxide-voltage definition does not yield a causal result.

IN-BAND ERRORS

We expect that errors in our calculated values of arg(p_+) will also create errors in $|Z_0'|$, the value of $|Z_0|$ we calculate from arg(p_0). Since the Hilbert transform is unitary, the root-mean-square (RMS) error in ln $|Z_0'|$ is the same as the RMS error in arg(p_+). Although small pointwise errors in arg(p_+) do not always imply small pointwise errors in $|Z_0'|$, we might guess that if the error in our calculations of arg($p_+(\omega)$) had a Gaussian distribution with standard deviation σ, then the errors in our calculations of ln $|Z_0'(\omega)|$ might also have a Gaussian distribution with the same standard deviation.

For comparison purposes, we first choose λ so that the average value of ln $|Z_0'/Z_0|$ is 0. To accomplish this we chose λ with

$$\ln\lambda \equiv -\frac{1}{N}\sum_i \ln\left|\frac{e^{-\mathcal{H}(\arg[p_+(\omega)])}}{Z_0(\omega_i)}\right|, \qquad \textbf{(7)}$$

where ω_i are the N frequencies at which we calculated $|Z_0|$. Next, we hypothesize that if the errors in arg(p_+) are normally distributed with mean 0 and standard deviation σ, then the errors Δ ln$|Z_0'|$ in ln$|Z_0'|$ will also be approximately normally distributed with mean 0 and standard deviation σ. Finally, if σ is small we expect $\Delta|Z_0|/|Z_0| \approx \Delta \ln|Z_0'|$, where $\Delta|Z_0| \equiv |Z_0'| - |Z_0|$.

We performed a Monte-Carlo experiment that supports this hypothesis. In the experiment we recalculated $|Z_0|$ twenty times, each time adding random phase errors of Gausian distribution (σ = 0.0175 radians) to our calculated values of arg(p_+).

Figure 2 compares 2σ, an estimate of the 95% confidence interval for $\Delta|Z_0|/|Z_0|$ (long dashes), and the sum of **(6)** for ω_0 = 150 GHz and 2σ (solid line) to the deviations we observed in the Monte-Carlo experiment. The figure shows the differences between our initial calculation of $|Z_0|$ performed with unperturbed data

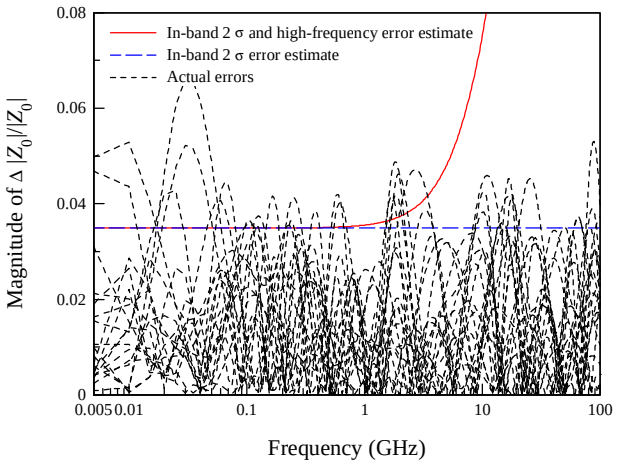

Fig. 2. Comparison of actual deviations in our Monte-Carlo experiment, the in-band 2σ estimate, and the sum of the in-band estimate and the high-frequency error bound.

and our calculations with perturbed data. The figure shows that the standard deviation of $\arg(p_+)$ does indeed provide a reasonable estimate of the average magnitudes of errors in Z_0 due to local errors in $\arg(p_+)$.

Figure 3 supports the hypothesis that the distribution of the relative errors $\Delta|Z_0|/|Z_0|$ is Gaussian. It compares the actual errors in $|Z_0|$ in our Monte-Carlo experiment to a Gausian distribution with a standard deviation σ of 0.0175. In particular, we found that 64% of our deviations fell within the region $\Delta|Z_0|/|Z_0| < \sigma$, and 94% within the region $\Delta|Z_0|/|Z_0| < 2\sigma$. These compare well with the 68 and 95 percentage points we expect from a true Gaussian distribution.

CONCLUSION

We developed an algorithm for calculating the magnitude of the characteristic impedance required by the causal power-normalized waveguide circuit theory of [1] and estimated its uncertainties.

SOFTWARE

We have posted the software we developed to calculate the causal magnitude of Z_0 from $\arg(p_+)$ on www.boulder.nist.gov/div813/dylan.

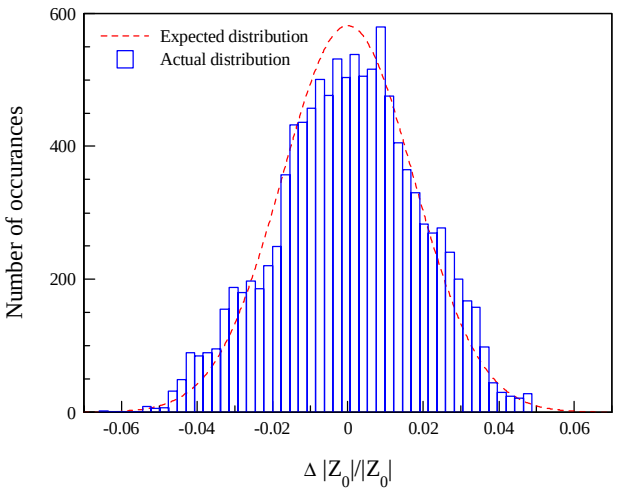

Fig. 3. Comparison of the actual distribution of errors in our Monte-Carlo experiment to the expected Gaussian distribution.

REFERENCES

[1] D.F. Williams and B.K. Alpert, "Causality and waveguide circuit theory," submitted to *IEEE Trans. Microwave Theory Tech.* Advance copies posted on http://www.boulder.nist.gov/div813/dylan/ and http://www.boulder.nist.gov/math/alpert.

[2] W. Heinrich, "Full-wave analysis of conductor losses on MMIC transmission lines," *IEEE Trans. Microwave Theory Tech.*, vol. MTT-38, no. 10, pp. 1468-1472, Oct. 1990.

[3] R. B. Marks and D. F. Williams, "A general waveguide circuit theory," *J. Res. Natl. Inst. Stand. Technol.*, vol. 97, no. 5, pp. 533-562, Sept.-Oct., 1992.

[4] N. Fache, F. Olyslager, and D. de Zutter, *Electromagnetic and Circuit Modeling of Multiconductor Transmission Lines*. Clarendon Press: Oxford, 1993.

[5] D.F. Williams and B.K. Alpert, "Characteristic impedance, power, and causality," *IEEE Microwave and Guided Wave Lett.*, vol. 9, no. 5, pp. 181-182, May 1999.

[6] D.F. Williams and B.K. Alpert, "Characteristic impedance of microstrip on silicon," *8th IEEE Electrical Performance of Electronic Packaging Conf. Dig.*, pp. 181-184, San Diego, CA, Oct. 25-27, 1999.

[7] Bateman Manuscript Project, *Tables of Integral Transforms*. McGraw-Hill: New York, 1954, Table 15.2 (8).